OTEM: Optimized Thermal and Energy Management for Hybrid Electrical Energy Storage in Electric Vehicles

Korosh Vatanparvar, Mohammad Abdullah Al Faruque
Department of Electrical Engineering and Computer Science
University of California, Irvine, California, USA
{kvatanpa, alfaruqu}@uci.edu

***Abstract*—Electric Vehicles (EV) pose challenges in terms of reliability and performance which are due to the stringent design constraints. For instance, an insufficient energy storage restricts the EV driving range. Highly dense battery packs providing EV with the required power, may generate extreme internal heat which causes the battery temperature to rise significantly and thereby results in reliability and safety issues. Moreover, both high battery utilization and temperature may degrade the battery capacity and Battery LifeTime (BLT), which should be extended as much as possible to postpone expensive battery replacement costs. Although, researchers have provided separate battery energy and thermal managements for EVs to address the above-mentioned challenges, in this paper, we are bringing a joint optimized solution. Hence, we introduce a novel metric Thermal and Energy Budget (TEB) in a Hybrid Electrical Energy Storage (HEES) with an active battery cooling system. Furthermore, we propose a novel Optimized Thermal and Energy Management (OTEM) methodology which optimizes the battery/ultracapacitor utilization, battery temperature, and thereby TEB, in order to improve the driving range, extend the BLT, and maintain the battery temperature in the safe zone. Our methodology provides significant improvement in BLT (on average 16.8%) and average energy consumption (on average 12.1% reduction) compared to the state-of-the-art methodologies.**

I. Introduction and Related Works

Electric Vehicles (EV) have been accepted as a sustainable solution and a new paradigm of transportation [1, 2] to address the environmental issues caused by greenhouse gases and other pollutants coming from road transportation. Despite the incentives provided by governments to promote EV deployment [3], EVs pose challenges of trade-off between cost and performance [4]. The cost, volume, and weight constraints in battery pack design make them the major bottleneck restricting the amount of energy stored for driving [5]. Besides driving range issue, the battery capacity degrades in long-term until it becomes useless after 20% of capacity loss [6]. Since battery production requires complex process and expensive material, the battery replacement gets sophisticated and costly which may cause economic and sustainability issues [7].

Hence, researchers have tried to extend the driving range and the Battery LifeTime (BLT) or operational time considering the design constraints; more efficient materials have been used in the batteries to provide more energy density, e.g. Li-ion batteries [8]. Sophisticated Battery Management Systems (BMS) with the capability of energy management have been implemented to utilize the battery more efficiently by monitoring its status, while meeting the safety requirements, e.g. thermal and power limits, and preventing over-charging and over-discharging [9–12]. To further improve the energy efficiency, Hybrid Electrical Energy Storage (HEES) [3, 13, 14] design has been introduced which may comprise of batteries and ultracapacitors connected in different architectures, e.g. parallel [15] or dual [16]. In HEES design, pulsed loads may be redirected to ultracapacitors which have higher power density [15] to improve the total energy efficiency. Since the battery capacity loss is significantly dependent on the battery operating temperature, decreasing the battery temperature may reduce its capacity loss thus extending the BLT [6, 16]. Hence, HEES has been also used to alleviate the thermal issues [17] caused by the heat generated from the battery cells [16].

A. Motivational Case Study for Thermal Management

We have conducted experiments to further analyze the performance of battery thermal managements. In this case study, the ultracapacitors are used when the temperature of battery cells reaches a certain threshold [16]. Fig. 1 illustrates the thermal management performance using an HEES for different ultracapacitor sizes. As shown in the figure, the temperature can be maintained using large ultracapacitors, however, the safe threshold for the battery cells' temperature may get violated while using smaller ultracapacitors. If the ultracapacitors' capacity is not sufficient, they will deplete before the batteries are cooled down well enough. Also, the batteries are required to recharge the ultracapacitors again, which may increase the battery temperature further than before in some circumstances. This will cause drastic battery capacity loss and decrease in BLT.

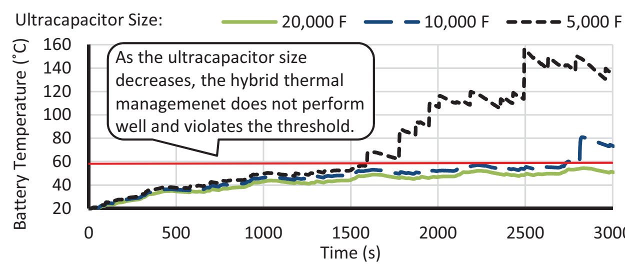

Fig. 1. Battery Cells' Temperature while Driving an EV Simulated in ADVISOR (Advanced Vehicular Simulator) for US06 Drive Cycle [16, 18].

Summary and conclusion from observations: the above analysis shows that ultracapacitors may not suffice to maintain the battery temperature and may not be a reliable solution for avoiding thermal issues (unsafe states). On the other hand, adding more ultracapacitors may significantly increase the HEES cost ($\approx \$12,000$ for $20,000F$) [19], volume, and mass which are constrained during the design time [20]. Hence, having an active battery cooling system is necessary for the energy storage in order to prevent thermal violations.

Moreover, the above-mentioned energy managements and BMSs have not considered the battery energy efficiency in different temperatures; it has been shown that Li-ion battery cells have higher usable capacity in higher temperatures [21]. On the other hand, the influence of ultracapacitors' high voltage swing on the HEES energy efficiency needs to be considered; power efficiency of the DC/DC converter used for the ultracapacitors may decrease as the voltage of the ultracapacitors drop while being overused [4, 13, 22]. Knowing these characteristics will help the thermal and energy management in BMS efficiently manage the energy among the batteries or ultracapacitors. Since the active battery cooling system consumes power to maintain the battery temperature, this Optimized Thermal and Energy Management (OTEM) has to know when to use the active battery cooling system or the ultracapacitors such that it improves the driving range, extends the BLT, and maintains the battery temperature in the safe range [16]. Furthermore, when OTEM decides to utilize the ultracapacitors, it needs to make sure there is enough charge allocated in them. On the other hand, when OTEM decides to utilize the battery, it needs to make sure the battery is cooled enough. In this paper, this quality metric is termed as Thermal and Energy Budget (TEB). The OTEM should provide enough TEB, i.e. pre-cool battery or pre-charge ultracapacitors, efficiently before utilizing the HEES.

B. Problem and Research Challenges

The problem of controlling the battery temperature and energy consumption for improving the driving range and battery lifetime poses the following key challenges:

1) Considering the HEES design combined with active battery cooling system for the thermal and energy management.
2) Accounting the total energy efficiency and battery lifetime while controlling the energy consumption and maintaining the temperature constraints.
3) Having an efficient and reliable methodology to avoid the thermal and energy violations while utilizing HEES.

C. Our Novel Contributions and Concept Review

To address the above-mentioned challenges, a novel HEES thermal and energy management methodology for improving the driving range and extending the battery lifetime is provided which employs:

1) **Hybrid Electrical Energy Storage (Section II):** in which the detailed electrical and thermal characteristics of the battery, ultracapacitor, and hybrid architectures are modeled and estimated.
2) **Active Battery Cooling System (Section II-D):** in which the thermal dynamics, power consumption, and influence on the battery temperature are modeled and estimated.
3) **Optimized Thermal and Energy Management (Section III):** which provides enough TEB for the HEES by optimizing the utilization of different energy storage and active battery cooling system power. The controller may pre-charge the ultracapacitor or pre-cool the battery efficiently upto the perfect amount, in order to extend the BLT, improve HEES efficiency, and minimize the energy consumption while maintaining the thermal constraints. This methodology is formulated using Model Predictive Control (MPC) [11, 23] in Section III-B.

Fig. 2 further describes our optimized thermal and energy management methodology for HEES. Different architectures for HEES design and ultracapacitor sizing are analyzed in Sections II and IV. Although the design space exploration for the HEES and active battery cooling system in terms of size and cost [5, 24, 25] is out of the scope of this paper, the methodology will be economical for any design variation.

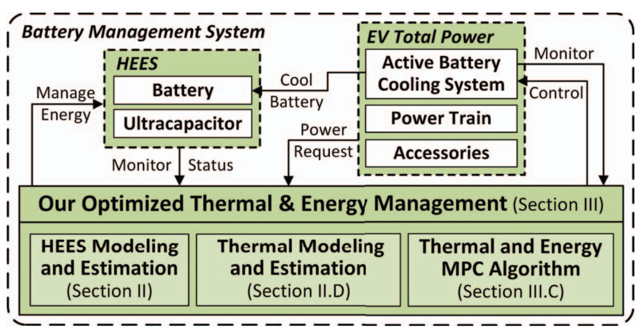

Fig. 2. Optimized Thermal and Energy Management Methodology for HEES.

II. System Modeling and Estimation

More knowledge about the future will help our OTEM to provide adequate TEB and control the components efficiently. Hence, the contributing components, e.g. battery, ultracapacitor, and active battery cooling system, are modeled to provide the OTEM (see Section III) with sufficient estimation of their behaviors; an EV power train and its drive cycle have been modeled in ADVISOR [18], in order to estimate the power requests from the EV. The power requests are then handled by the controller in OTEM (see Section III-C). An optimized MPC algorithm will monitor and control the HEES (see Section II-C) comprising of batteries (see Section II-A) and ultracapacitors (see Section II-B), and the active battery cooling system (see Section II-D).

A. Battery Model

Battery packs are designed according to the requirements specified for each EV. Typically, EVs deploy Li-ion battery cells as their primary electrical energy storage [4]. For instance, Tesla Model S utilizes a battery pack made out of 18650A battery cells [21, 26]. Although, the electrical and thermal characteristics of these cells vary for each type, the Li-ion battery cells used for EVs (18650A), are mostly modeled as the following.

Electrical model for each battery cell is described using an equivalent electric circuit model [16]; the battery cell is modeled as a variable voltage power supply in series with an internal resistance (see Fig. 3 and 4). The ratio of the available charge to the battery capacity is represented by State-of-Charge (SoC). Open-circuit voltage (V_{OC}) of the battery (the variable voltage power supply) and the battery internal resistance (R_{bat}) depend on SoC value, which are modeled by:

$$SoC_t = SoC_0 - 100 \times \int_0^t \frac{I_{bat}}{C_{bat}} \tag{1}$$

$$V_{OC} = v_1 e^{v_2 SoC_t} + v_3 SoC_t^4 + v_4 SoC_t^3 \\ + v_5 SoC_t^2 + v_6 SoC_t + v_7 \tag{2}$$

$$R_{bat} = r_1 e^{r_2 SoC_t} + r_3 \tag{3}$$

where C_{bat} is the rated battery capacity (in Ah) evaluated in nominal discharge rate [21]. I_{bat} is the current drawn from the battery. SoC_0 represents the initial SoC at time 0. v_x and r_x parameters can be empirically measured for each specific battery type [16, 21].

The energy production by a battery depends on its chemical metabolism and internal resistance which change by the operating temperature; elevated battery temperature improves the energy production by lowering the internal resistance and speeding up the chemical metabolism. This behavior is modeled as temperature-sensitive r_x parameters in Eq. 3. The value for this parameter can be extracted from the battery manufacturer's datasheet [21].

Li-ion batteries generate internal heat (Q_{bat}) while charging/discharging. The heat generated is caused by the power loss due to the internal resistance or the entropy change in the ions [16, 25]. Based on the current battery utilization, the heat generated from each battery is approximated using:

$$Q_{bat} = I_{bat}(V_{OC} - V_{bat}) + I_{bat} T_{bat} \frac{dV_{OC}}{dT_{bat}} \tag{4}$$

where V_{bat} is the battery terminal voltage (which may be measured under load), T_{bat} is the current battery temperature, and $\frac{dV_{OC}}{dT_{bat}}$ is a constant for approximating the entropy change influence on the heat generated. The values for these parameters can be empirically measured for each specific battery type [16]. It needs to be noted that although more detailed battery electrical model may increase behavior modeling accuracy, it will not contradict our methodology.

The internal heat generated from each battery will increase the battery temperature. A battery may be comprised of multiple materials with different density and thermal characteristics [25]. A thermal capacity variable (C_b) in a **thermal model** is used to approximate the changing temperature behavior regarding the internal heat and the convection heat from the environment, e.g. air or active battery cooling system. HEES thermal behaviors are modeled with details in Section II-D.

The battery capacity degrades over time based on the battery utilization. Battery stress, number of discharge cycles, discharge current, and temperature influence the capacity loss [6]. In this paper, the capacity loss is modeled considering the discharge current and temperature:

$$Q_{loss} = l_1 e^{-l_2/(RT_{bat})} I_{bat}^{l_3} \tag{5}$$

where R is the ideal gas constant. l_x parameters are the coefficients in the model that can be measured empirically [6, 16].

B. Ultracapacitor Model

Ultracapacitors are used as secondary energy storage for EVs [4]. Since ultracapacitors unlike batteries do not conduct chemical reactions to provide electrical energy, they can be charged/discharged faster than batteries. Due to their higher power density, they are used in parallel with batteries to handle the high-rate pulsed load [15]. Ultracapacitors are modeled as a variable voltage power supply and an internal resistance [15] (see Fig. 3 and 4). Ratio of the available energy stored in an ultracapacitor to its energy capacity (maximum energy that can be stored - E_{cap}) is represented by State-of-Energy (*SoE*). The voltage across the ultracapacitor (V_{cap}) varies significantly with the *SoE*. The **electrical model** is described as follows:

$$E_{cap} = 1/2\ C_{cap} V_r^2 \tag{6}$$

$$I_{cap} = C_{cap}\ dV_{cap}/dt \tag{7}$$

$$V_{cap} = V_r \sqrt{SoE_t/100} \tag{8}$$

$$SoE_t = SoE_0 - 100 \times \int_0^t \frac{V_{cap} I_{cap}}{E_{cap}} \tag{9}$$

where C_{cap} is the rated capacitance [19], V_r is the rated voltage of the ultracapacitor, I_{cap} is the current drawn from the ultracapacitor. SoE_0 represents the initial *SoE* at time 0. Since the internal resistance of an ultracapacitor is very inconsiderable ($\approx 2.2m\Omega$), it has been omitted in the model. Also, because ultracapacitors do not generate considerable heat, we can ignore them in the **thermal model**.

C. Hybrid Electrical Energy Storage Model

HEES design is composed of multiple battery cells and ultracapacitors. There are different hybrid architectures in the literature defining the way of connecting and managing the energy storage:

1) **Dual/Parallel:** as shown in Fig. 3, in this architecture which was recently used for thermal management in [16], two switches (S_b, S_c) are used to change the connection to the battery or the ultracapacitor. In the dual architecture, the battery and the ultracapacitor can be connected in parallel or individually to the EV (see Fig. 3). When each energy storage is connected individually to the EV, the electrical model is described using the equations defined in Sections II-A and II-B. Otherwise, when they are connected in parallel, we use the following equations [16]:

$$P_l = V_l I_l \tag{10}$$

$$I_l = I_b + I_c \tag{11}$$

$$V_l = V_b - R_b I_b \tag{12}$$

$$V_l = V_c - R_c I_c \tag{13}$$

where P_l, I_l ,and V_l are the load requested by the EV, the current drawn from the HEES, and the voltage output to the load, respectively. V_b, R_b, and I_b are the open-circuit voltage, the internal resistance, and the current drawn for the total battery pack (see Section II-A). V_c, R_c, and I_c are the open-circuit voltage, the internal resistance (it can be omitted), and the current drawn for the total ultracapacitor pack (see Section II-B).

2) **Hybrid:** as shown in Fig. 4, in this architecture, each energy storage is connected indirectly using a DC/DC converter to a DC bus in EV [3]. Hence, each energy storage can be independently used with the capability of energy migration and allocation [14]. This architecture is mainly used for our optimized HEES thermal and energy management, since it provides the flexibility to control the utilization of each energy storage.

Performance of the DC/DC converters used for the energy storage changes for various voltages. As the voltage domain drops, the conversion efficiency decreases. Hence, the conversion efficiency is modeled as a parameter η_{DC}, which affects the power requests to the ultracapacitors, batteries, or the dual/parallel architecture. The value for this parameter can be measured empirically [22].

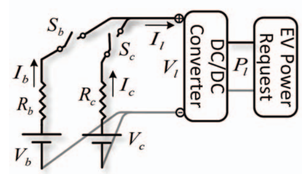

Fig. 3. Dual/Parallel Architecture

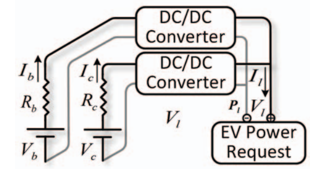

Fig. 4. Hybrid Architecture

D. Active Battery Cooling System Model

Although the heat generated from the batteries are significantly dependent on the EV and the battery type (see Section II-A), having energy-dense and high-power batteries necessitate the existence of a methodology to prevent over-heating. Recently, EVs utilize active battery cooling system to maintain the battery temperature in the safe range. Another approach is through constraining the battery utilization by redirecting the power to another energy storage - ultracapacitor - as in [16]. However, as shown in Section I, HEES is not sufficient for preventing the battery over-heating and the active battery cooling system is necessary to maintain the battery performance and reliability.

As stated in Section II-A, the battery cells are connected together in parallel or series inside a battery pack (see Fig. 5). In the existence of an active battery cooling system, the battery cells are surrounded by a flowing coolant. The coolant may be gas or liquid depending on the configuration. However, the coolant material is orthogonal to the methodology provided and may only change the parameter values for the equations, we have considered the details for the coolant as in [25]. The coolant is pumped to the battery pack using an electric motor (pump). The hot coolant returned from the battery pack is cooled down by a cooler and pumped back to the system again. Since the ultracapacitors do not generate considerable internal heat, they are not considered in the cooling system and they may be packed separately from the battery pack.

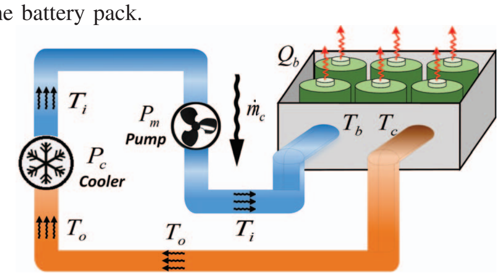

Fig. 5. Active Battery Cooling System for the Battery Pack.

The battery temperature (T_b) is influenced by the internal heat generated from the battery (Q_b) and the heat exchange with the coolant. Since the battery pack is completely isolated from outside, the ambient temperature does not influence the battery temperature directly. The energy balance for a battery cell is described as:

$$C_b \frac{dT_b}{dt} = h_{cb}(T_c - T_b) + Q_b \tag{14}$$

where C_b is the battery cell heat capacity (see Section II-A), h_{cb} is the heat transfer coefficient between the coolant and the battery, and T_c is the coolant temperature in the battery pack. Hence, the battery temperature changing rate ($\frac{dT_b}{dt}$) can be evaluated using Eq. 14.

The coolant temperature inside the battery pack (T_c) is influenced by the heat exchange with the battery cells and the coolant pumped to the battery pack. Since the battery cells are small, we can simplify the heat exchange model between the battery and coolant further without affecting the concept of the paper. Hence, both the battery cells and the coolant are lump modeled by their heat capacity. The energy balance for the coolant is described as:

$$C_c \frac{dT_c}{dt} = h_{bc}(T_b - T_c) + C_c(T_i - T_c) \tag{15}$$

where C_c is the coolant heat capacity [25] and h_{bc} is the heat transfer coefficient between the coolant and the battery. Hence, the coolant temperature changing rate ($\frac{dT_c}{dt}$) can be evaluated using Eq. 15.

The coolant returned from the battery pack is cooled down by a cooler. The cooler power consumption (P_c) is proportional to the energy difference between its inlet and outlet coolant flow. Moreover, the heat exchange among the coolant, environment air, and potential secondary coolant in the cooling system is modeled as an efficiency parameter (η_c), which is influenced by the operating conditions.

$$P_c = \frac{C_c}{\eta_c}(T_o - T_i) \tag{16}$$

The pump is needed for maintaining the coolant flow rate. The pump power consumption (P_m) is related to the coolant flow rate ($\dot{m}_c$). In this paper, the coolant flow rate is considered fixed which makes the pump power consumption a constant.

III. Thermal and Energy Management

In the previous sections, battery (see Section II-A), ultracapacitor (see Section II-B), and HEES design (see Section II-C) have been modeled in order to estimate their electrical and thermal characteristics, e.g., energy consumption, battery lifetime, and generated internal heat. This information is leveraged by our OTEM to maintain the battery temperature, extend the battery lifetime, reduce the energy consumption by the active battery cooling system, and improve the energy efficiency of the HEES (reducing the energy loss in battery, ultracapacitor, or DC/DC converters).

A. Methodology Description

In OTEM, based on the models of the components contributing to the system, we may predict the future state of the system for defined period of time (control window). Knowing more information about the future may help the controller to configure and utilize the system, e.g. HEES, in a more desirable and efficient way while minimizing a cost function, e.g. improve the BLT and reduce the energy consumption/loss. This method of controlling is known as Model Predictive Control (MPC) [11, 23].

The novelty of this methodology is to simultaneously consider the battery temperature, energy consumption of active battery cooling system, and energy consumed (including energy loss) in the HEES while considering the energy efficiency in different conditions. These values are estimated for a time period in future. Hence, the OTEM provides sufficient TEB before the EV power requests arrive. And, the HEES will be at the most efficient state for handling the power requests.

B. Optimization Formulation

Since the controlling is conducted in discrete time, the model equations need to be also discretized. For instance, Eq. 15 which models the thermal behavior of the battery, is defined in discrete time as follows:

$$C_b \frac{T_b^+ - T_b}{\triangle t} = h_{cb}\left(\frac{T_c^+ + T_c}{2} - \frac{T_b^+ + T_b}{2}\right) + Q_b \tag{17}$$

where "+" symbol represents the value of the variable at the next time step $t + \triangle t$. Here, $\triangle t$ is the time step duration (sampling period).

The EV power request predicted by modeling the power train and driving route [3] is passed as an input variable to the controller. Let P_e^t be the estimated EV power consumption at time t. In the OTEM, let $x^{k|t}$ be the value of the state variables vector $[T_b, T_c, SoE, SoC]$, $i^{k|t}$ be the value of the controlling input variables vector $[T_i, P_{bat}, P_{cap}]$, and $u^{k|t}$ be the value of the auxiliary variables vector $[P_e, P_c, Q_{loss}, T_o, dE_{bat}, dE_{cap}]$ at time $t + k \triangle t$, predicted at time t.

The control requirements and physical restrictions state the following inequality constraints on state variables, controlling input variables, and auxiliary variables:

C1: $\underline{T_b} \leq T_b \leq \overline{T_b}$ safety restrictions on battery temperature
C2: $\underline{T_i} \leq T_o$ cooler always decreases the temperature
C3: $P_c \leq \overline{P_c}$ cooler maximum power output
C4: $20\% \leq SoC \leq 100\%$ charge restriction on battery
C5: $20\% \leq SoE \leq 100\%$ energy restriction on ultracapacitor
C6: $P_{bat} \leq \overline{P_{bat}}$ battery power restriction
C7: $P_{cap} \leq \overline{P_{cap}}$ ultracapacitor power restriction

The discrete-time model equations, system dynamics are defined as the equality constraints (C_{eq}) for the optimization process of the controller. Moreover, initial conditions for the state variables are dictated using equality constraints. For instance, the initial value of T_b to estimate $T_b^{k+1|t}$ should be equal to $T_b^{k|t}$. $T_b^{0|t+1}$ should be equal to estimated T_b^+ at time t:

$$C_{eq}^j\left(\begin{bmatrix} x^{k|t} \\ i^{k|t} \\ u^{k|t} \\ x^{k+1|t} \end{bmatrix}\right) = 0 \qquad C^i \begin{bmatrix} x^{k|t} \\ i^{k|t} \\ u^{k|t} \\ x^{k+1|t} \end{bmatrix} \leq b^i \tag{18}$$

where C_{eq}^j is a non-linear function describing the equality constraints. C^i and b^i are matrices stating the linear inequality constraints.

Our OTEM mainly attempts to decrease the energy consumption by the active battery cooling system, energy consumption/loss in the HEES, and battery capacity loss. This goal is represented by the following cost function which needs to be minimized:

$$F = \sum_{\tau=t}^{t+N\triangle t} w_1(P_c \triangle t) + w_2 Q_{loss} + w_3(dE_{bat} + dE_{cap}) \tag{19}$$

where N is the MPC control window size. w_1 represents the weight for reducing the active battery cooling power consumption (P_c), w_2 represents the weight for reducing the capacity loss (Q_{loss}) in the battery in order to improve its BLT, and w_3 represents the weight for reducing the energy used from the HEES which is the sum of energy consumed/lost in the battery and the ultracapacitor. The values of these variables in the MPC control window are summed as the cost.

C. Control Algorithm

The optimized thermal and energy management system monitors and controls the components at the driving-time. Using the estimated values by the implemented models, the optimization problem (see Eq. 18 and 19) is solved at each instances of time.

Algorithm 1 is the pseudo-code representing the methodology used in our OTEM. The estimated values for EV power requests are added as vector $\widehat{P_e}$. The driving duration is saved as T and two variables Q_{loss} and *Energy* are defined to store the values for capacity loss in battery and energy consumed in HEES, respectively (lines 1-3). The size of the control window for MPC algorithm is defined in line 4. The state variables (x, x^+), control input variables (i), and auxiliary variables (u) for the control window are defined (lines 5-8). The initial conditions for the state variables at time zero are defined in line 9. The for-loop in lines 10-22 represents the driving-time thermal and energy management. In lines 11 and 12, the estimated values for EV power requests during the control window are initialized. These state, control input, and auxiliary variables are combined in a vector as optimization variables (z) (lines 13). The optimization variables are passed to the solver to solve the optimization problem defined in Eq. 18 and 19 (line 14). The optimized values will be passed to the package (containing active battery cooling system and

Algorithm 1: Our Optimized Thermal and Energy Management

Input: Estimated Power Request $\widehat{P_e} = \{P_e^t \mid 0 \leq t \leq T\}$
Output: Measured Capacity Lost in Battery Q_{loss}
Output: Measured Energy Consumed in HEES *Energy*
`// the total route duration`
1 T = length $(\widehat{P_e})$
2 $Q_{loss} = 0$
3 $Energy = 0$
4 N = control window duration
5 $x = N \times 4$ matrix `// state variable`
6 $i = N \times 3$ matrix `// control inputs`
7 $u = N \times 6$ matrix `// auxiliary variables`
8 $x^+ = N \times 4$ matrix `// state variable`
9 $x^0 \leftarrow [298, 298, 100, 100]$ `// initial conditions`
`// driving-time thermal and energy management`
10 **for** $t = 1$ *to* T **do**
11 **for** $\tau = 0$ *to* $N - 1$ **do**
12 $u^\tau[P_e] \leftarrow P_e^{\tau+t}$
`// control window optimization variables`
13 $z \leftarrow [x, i, u, x^+]$
14 z_{opt} = Optimize (z) `// call optimizer`
`// apply control inputs & measure the states`
15 $[T_b^+, T_c^+, P_c]$ = Package (z_{opt})
16 $[SoC^+, SoE^+, dE_{bat}, dE_{cap}, Q_l]$ = HEES (z_{opt})
`// accumulate the capacity loss in battery`
17 $Q_{loss} \leftarrow Q_{loss} + Q_l$
`// accumulate the energy consumed in HEES`
18 $Energy \leftarrow Energy + dE_{bat} + dE_{cap}$
19 $x^0[T_b] \leftarrow T_b^+$ `// next time step initial` T_b
20 $x^0[T_c] \leftarrow T_c^+$ `// next time step initial` T_c
21 $x^0[SoC] \leftarrow SoC^+$ `// next time step initial` SoC
22 $x^0[SoE] \leftarrow SoE^+$ `// next time step initial` SoE
23 **return** $[Q_{loss}, Energy]$

the battery pack) for thermal management and the HEES for energy management and the outcome states are evaluated (lines 17-18). The capacity loss in the battery and energy consumed in the HEES are estimated and accumulated in Q_{loss} and *Energy*, respectively (lines 17-18). The estimated values of the state variables in this time step will be used as the initial conditions for the next time step (lines 19-22). Eventually, the values of Q_{loss} and *Energy* are returned.

IV. Experimental Results

A. Experimental Setup

The model equations defined in Section II contain multiple parameters which are mostly defined by the real-life specifications of the system. The values of the parameters are set and adjusted so that the system dynamics are verified by the experimental data gathered from the existing references. Our OTEM methodology defined in Section III is implemented in MATLAB/Simulink [27] and the EV power consumption is estimated using ADVISOR (Advanced Vehicular Simulator) [18]. For evaluation, we use multiple standard driving cycles [12] as the driving routes, different environment temperatures, and conduct the simulation using these two platforms.

B. Comparison to State-of-the-Art

We compare our optimized thermal and energy management methodology with:

1) ***Parallel Architecture [15]:*** where the simple parallel architecture (Section II-C) is used in the HEES design. There is no thermal or energy management implemented.
2) ***Active Battery Cooling System [25]:*** where only battery is used as the energy storage and active battery cooling system is utilized to maintain the battery temperature in the safe range.
3) ***Dual Architecture [16]:*** where the dual architecture with switches (Section II-C) is used in the HEES design in order to maintain the battery temperature by switching to ultracapacitor.

For fairness of the comparisons, all methodologies have been applied for the same system configuration, drive cycle, and physical restriction (unless otherwise specified).

1) Battery Temperature Analysis: the battery temperature has been monitored for the listed methodologies. As shown in Fig. 6, the dual architecture methodology reacts when the battery temperature reaches a threshold, in which may not be sufficient for extending BLT. However, the OTEM attempts to decrease the battery temperature further by managing the utilization of different energy storage and the cooler in order to extend the battery lifetime.

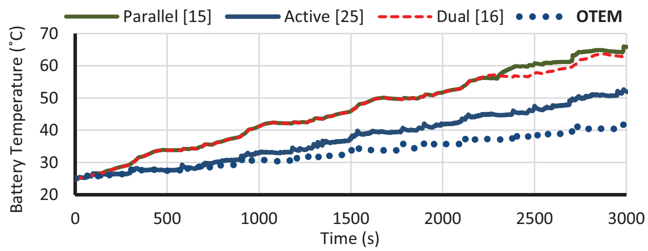

Fig. 6. Battery Temperature Analysis for Different Methodologies.

To further analyze the OTEM methodology, we have performed the temporal analysis on the battery temperature, the ultracapacitor *SoE*, and the EV power requests. As shown in Fig. 7, the OTEM provides enough TEB when it notices large EV power requests in the near-future; it allocates more charge to the ultracapacitor or cools the battery to the right amount so that the HEES stays in the most efficient state. This will decrease the capacity loss and increase the energy efficiency of the HEES. Analyses shown in Fig. 6 and 7 have been done using $25,000F$ ultracapacitors and driving in US06 five times.

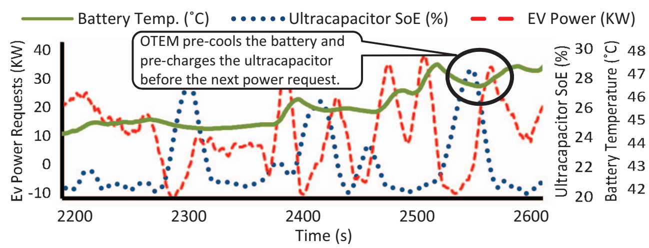

Fig. 7. Illustrating the TEB preparation for the HEES using the OTEM.

2) Battery Lifetime Analysis: the EV has been driven for multiple drive cycles under control by different methodologies and the battery capacity loss has been monitored and compared. Fig. 8 illustrates the ratio of the battery capacity loss in each methodology compared to the parallel architecture methodology. The OTEM decreases the capacity loss by 16.38% on average compared to the parallel architecture methodology and by 11.3% on average compared to the dual architecture methodology. The performance of each methodology varies for different drive cycles, since the EV requires different amount of power and the battery may not get heated the same.

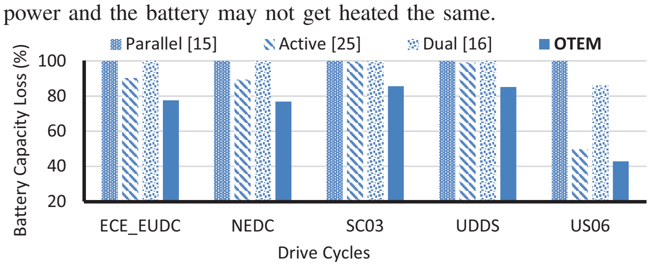

Fig. 8. Battery Lifetime Comparison for Different Methodologies in Multiple Drive Cycles.

3) Energy Consumption Analysis: as we have stated, the HEES energy efficiency depends significantly on the battery temperature and the ultracapacitor *SoE*. In Fig. 9, we have compared the average power consumption of the EV and the active battery cooling system (if available). As shown in the figure, the methodologies which use active battery cooling system have consumed more energy compared to others, since they attempt to decrease the battery temperature and extend BLT by cooling. However, in the OTEM, the average power consumption has been decreased by 12.1% on average compared to the pure active battery cooling system architecture, since HEES design has also contributed.

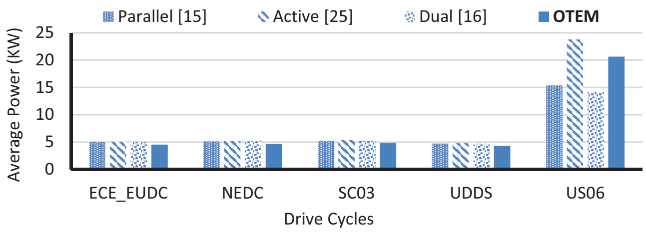

Fig. 9. Power Consumption Comparison for Different Methodologies in Multiple Drive Cycles.

4) Ultracapacitor Size Analysis: in previous analyses we have considered the ultracapacitor size fixed $(25,000F)$. However, the HEES efficiency and the methodologies' performance may vary significantly based on the ultracapacitor size. In Table I, we have illustrated the average power consumption and the capacity loss (compared to the parallel architecture using $25,000F$ ultracapacitor) for different ultracapacitor sizes controlled by different methodologies. The experiment has been done using the US06 drive cycle, since it is a highly power consuming drive cycle. The table shows that, by decreasing the ultracapacitor size, the average power consumption increases significantly in parallel and dual architectures. Also, the capacity loss while using the dual architecture increases by decreasing the size, since the methodology significantly depends on the ultracapacitor size. In the OTEM, the increase in the ultracapacitor size will help the efficiency of the HEES and the OTEM performance. However, since the OTEM has the flexibility of using active battery cooling system, it is not much dependent on the ultracapacitor size.

TABLE I. Analyzing the Influence of Ultracapacitor Size in Different Methodologies.

Ultracapacitor Sizes	Average Power (W)			Capacity Loss (%)		
	Parallel [15]	Dual [16]	**OTEM**	Parallel [15]	Dual [16]	**OTEM**
5,000 F	16,919	15,239	22,391	175.24	85.53	49.03
10,000 F	16,893	14,381	22,274	136.02	82.84	48.61
20,000 F	16,856	13,891	21,094	107.21	78.30	44.40
25,000 F	16,846	14,156	20,662	100.00	84.70	42.85

V. Conclusion

In literature, active battery cooling system or HEES has been considered as solutions to address the thermal issues influencing the battery performance and longevity. However, active battery cooling system alone may not be efficient for improving the EV driving range. And, the HEES alone is an unreliable and costly solution to maintain the battery temperature in the safe zone, which is highly dependent on the ultracapacitor size. Hence, in this paper, we have integrated both the solutions and implemented an OTEM methodology that provides optimized TEB for the HEES before handling the power requests; it may pre-charge the ultracapacitor or pre-cool the battery to put the HEES in the most efficient state. Our methodology demonstrates significant improvement in BLT (on average 16.8%) and average power consumption (on average 12.1% reduction) compared to the state-of-the-art methodologies. We have also shown that the decrease in the ultracapacitor size, which is preferable for HEES design, may not influence the OTEM performance.

References

[1] M. Lukasiewycz and S. Steinhorst, "System Architecture and Software Design for Electric Vehicles," *Proceedings of the Design Automation Conference (DAC'13)*, pp. 1–6, 2013.

[2] M. A. Al Faruque and K. Vatanparvar, "HVAC System and Automotive Climate Control Influence on Electric Vehicle and Battery," *Asia and South Pacific Design Automation Conference (ASP-DAC)*, pp. 1–6, 2016.

[3] S. Park, Y. Kim, and N. Chang, "Hybrid Energy Storage Systems and Battery Management for Electric Vehicles," *Proceedings of the Design Automation Conference (DAC'13)*, pp. 1–6, 2013.

[4] S. Chakraborty, M. Lukasiewycz *et al.*, "Embedded Systems and Software Challenges in Electric Vehicles," *Proceedings of the Conference on Design, Automation & Test in Europe (DATE'12)*, pp. 424–429, 2012.

[5] W. Chang, M. Lukasiewycz, S. Steinhorst, and S. Chakraborty, "Dimensioning and configuration of EES systems for electric vehicles with boundary-conditioned adaptive scalarization," *Proceedings of the International Conference on Hardware/Software Codesign and System Synthesis (CODES+ISSS'13)*, pp. 1–10, 2013.

[6] A. Millner, "Modeling Lithium Ion Battery degradation in electric vehicles," *IEEE Conference on Innovative Technologies for an Efficient and Reliable Electricity Supply*, pp. 349–356, 2010.

[7] S. B. Peterson, J. F. Whitacre, and J. Apt, "The economics of using plug-in hybrid electric vehicle battery packs for grid storage," *Journal of Power Sources*, vol. 195, no. 8, pp. 2377–2384, 2010.

[8] F. R. Kalhammer, B. M. Kopf, D. H. Swan, V. P. Roan, and M. P. Walsh, "Status and Prospects for Zero Emissions Vehicle Technology," *Report of the ARB Independent Expert Panel*, p. 25, 2007.

[9] L. Lu, X. Han, J. Li, J. Hua, and M. Ouyang, "A review on the key issues for lithium-ion battery management in electric vehicles," *Journal of Power Sources*, pp. 272–288, 2013.

[10] K. W. E. Cheng, B. P. Divakar, H. Wu, K. Ding, and H. F. Ho, "Battery-management system (BMS) and SOC development for electrical vehicles," *IEEE Transactions on Vehicular Technology*, pp. 76–88, 2011.

[11] K. Vatanparvar and M. A. Al Faruque, "Battery Lifetime-Aware Automotive Climate Control for Electric Vehicles," *Proceedings of the Design Automation Conference (DAC'15)*, pp. 1–6, 2015.

[12] K. Vatanparvar, J. Wan, and M. A. Al Faruque, "Battery-Aware Energy-Optimal Electric Vehicle Driving Management," *International Symposium on Low Power Electronics and Design (ISLPED)*, pp. 353–358, 2015.

[13] M. Pedram, N. Chang, Y. Kim, and Y. Wang, "Hybrid electrical energy storage systems," *Proceedings of the 16th International Symposium on Low Power Electronics and Design (ISLPED'10)*, p. 363, 2010.

[14] Q. Xie, Y. Wang *et al.*, "Charge allocation in hybrid electrical energy storage systems," *IEEE Transactions on Computer-Aided Design of Integrated Circuits and Systems*, pp. 1003–1016, 2013.

[15] D. Shin, Y. Kim *et al.*, "Battery-supercapacitor hybrid system for high-rate pulsed load applications," *Proceedings of the Conference on Design, Automation & Test in Europe (DATE'11)*, pp. 1–4, 2011.

[16] D. Shin, M. Poncino, and E. Macii, "Thermal Management of Batteries Using a Hybrid Supercapacitor Architecture," *Proceedings of the Conference on Design, Automation & Test in Europe (DATE'14)*, 2014.

[17] A. A. Pesaran, "Battery Thermal Management in EVs and HEVs: Issues and Solutions," *Advanced Automotive Battery Conference*, p. 10, 2001.

[18] K. B. Wipke, M. R. Cuddy, and S. D. Burch, "ADVISOR 2.1: A User-Friendly Advanced Powertrain Simulation Using a Combined Backward/Forward Approach," *IEEE Transactions on Vehicular Technology*, pp. 1751–1761, 1999.

[19] Maxwell "BC Series Ultracapacitors Datasheet". maxwell.com., 2015.

[20] J. Cao and A. Emadi, "A New Battery/UltraCapacitor Hybrid Energy Storage System for Electric, Hybrid, and Plug-in Hybrid Electric Vehicles," *IEEE Transactions on Power Electronics*, pp. 122–132, 2012.

[21] Panasonic "Lithium Ion NCR18650A Datasheet". industrial.panasonic.com/lecs/www-data/pdf2/ACA4000/ACA4000CE254.pdf., 2015.

[22] Y. Choi, N. Chang, and T. Kim, "DC-DC converter-aware power management for low-power embedded systems," *IEEE Transactions on Computer-Aided Design of Integrated Circuits and Systems*, 2007.

[23] E. F. Camacho and C. B. Alba, "Model predictive control," *Springer Science & Business Media*, 2013.

[24] A. Du Pasquier, I. Plitz *et al.*, "A comparative study of li-ion battery, supercapacitor and nonaqueous asymmetric hybrid devices for automotive applications," *Journal of Power Sources*, pp. 171–178, 2003.

[25] G. Karimi and X. Li, "Thermal management of lithium-ion batteries for electric vehicles," *Journal of Energy Research*, pp. 13–24, 2013.

[26] Tesla Motors Inc."Tesla Model S Spec". www.teslamotors.com., 2015.

[27] MathWorks "MATLAB, Simulink". www.mathworks.com., 2015.